IOP Publishing Semiconductor Science and Technology
Semicond. Sci. Technol. 29 (2014) 115025 (6pp) doi:10.1088/0268-1242/29/11/115025

Computational analysis of the maximum power point for GaAs sub-cells in InGaP/GaAs/Ge triple-junction space solar cells

M A Cappelletti[1,2], A P Cédola[1] and E L Peltzer y Blancá[1]

[1] Grupo de Estudio de Materiales y Dispositivos Electrónicos (GEMyDE), Dpto. de Electrotecnia, Facultad de Ingeniería, Universidad Nacional de La Plata, 48 y 116, CC.91, La Plata (1900), Argentina
[2] Universidad Nacional Arturo Jauretche, Avenida Calchaquí 6200, Florencio Varela (1888), Buenos Aires, Argentina

E-mail: marcelo.cappelletti@ing.unlp.edu.ar

Received 6 June 2014, revised 24 August 2014
Accepted for publication 5 September 2014
Published 2 October 2014

Abstract

The radiation resistance in InGaP/GaAs/Ge triple-junction solar cells is limited by that of the middle GaAs sub-cell. In this work, the electrical performance degradation of different GaAs sub-cells under 1 MeV electron irradiation at fluences below 4×10^{15} cm^{-2} has been analyzed by means of a computer simulation. The numerical simulations have been carried out using the one-dimensional device modeling program PC1D. The effects of the base and emitter carrier concentrations of the p- and n-type GaAs structures on the maximum power point have been researched using a radiative recombination lifetime, a damage constant for the minority carrier lifetime and carrier removal rate models. An analytical model has been proposed, which is useful to either determine the maximum exposure time or select the appropriate device in order to ensure that the electrical parameters of different GaAs sub-cells will have a satisfactory response to radiation since they will be kept above 80% with respect to the non-irradiated values.

Keywords: electron irradiation, maximum power point, solar cells, computer simulation

1. Introduction

The study of semiconductor devices that can provide power at a low operating cost, such as solar cells, is extremely important at the present time because they are being increasingly used in space power applications. Solar cells in space are exposed to the irradiation of high energy particles of the near-Earth space environment; this environment consists primarily of protons and/or electrons, which degrade the electrical performance of the devices [1, 2]. In the worst case scenario, these situations can lead to permanent mission failure. Recently, monolithic multi-junction solar cells (MJSC) based on III–V technologies, particularly the InGaP/GaAs/Ge triple-junction (3J), are the main power sources for spacecrafts since they have demonstrated higher conversion efficiencies and better radiation resistance compared to Si single crystalline and GaAs devices [3–6].

Understanding the radiation response of electronic components is essential to predict whether the devices and the whole system would work correctly during the expected mission lifetime. Every different solar cell structure from a given material is expected to respond differently with respect to the type and energy of the incident particles (protons, electrons, etc) and to the particular mission variables such as orbital altitude, inclination and elapsed time after launch [7]. Previous studies have reported that the top InGaP and the bottom Ge sub-cells in the InGaP/GaAs/Ge 3J solar cell are subjected at a lesser degree to radiation degradation; consequently, the radiation resistance is limited by that of the middle GaAs sub-cell [8, 9]. Therefore, further research in GaAs sub-cells with the aim of developing InGaP/GaAs/Ge 3J space solar cells with improved radiation resistance is still required.

In recent years, theoretical studies of Si PIN photodiodes and Si solar cells for use in space-radiation environments have allowed the authors to propose useful analytical models related to the structural characteristics of the devices in order to contribute to the design of radiation-hardened devices

 © 2014 IOP Publishing Ltd Printed in the UK

Table 1. Physical parameters used in the analysis.

Physical parameters at 300 K	Values
Electron mobility, μ_e	8500 $cm^2 V^{-1} s^{-1}$
Hole mobility, μ_h	400 $cm^2 V^{-1} s^{-1}$
Emitter thickness	0.5 μm (p-on-n GaAs)
Emitter thickness	0.15 μm (n-on-p GaAs)
Base thickness	3 μm
Dielectric constant	12.9
Band gap	1.424 eV
Intrinsic carrier concentration, n_i	2×106 cm^{-3}

[10–12]. Nowadays, efficient and accurate modeling and simulation techniques are fundamental tools to predict and propose new designs that will improve the response of electronic devices under different operation conditions at a much lower cost and in less time than experimental testing.

This work aims to continue the advancement in this research area. In this case, the performance of individual p-on-n and n-on-p GaAs sub-cells for InGaP/GaAs/Ge 3J solar cells under 1 MeV electron irradiation has been analyzed by means of computer simulation. The effects of both base and emitter carrier concentration upon the radiation resistance of these devices have been researched using a radiative recombination lifetime, a damage constant for the minority carrier lifetime and the carrier removal rate of GaAs for the purpose of understanding the influence of the design parameters on the maximum power point (P_{MPP}) of the solar cells. The P_{MPP} is the major design consideration of the electrical parameters in space solar cells. The numerical simulations have been carried out using the one-dimensional device modeling program PC1D [13].

2. Radiation damage model

The performance of solar cells used in space systems is degraded by the impact of high energy particles (protons, electrons, etc) that damage semiconductor structures, thereby accelerating the aging of the devices. Under these operating conditions, the most important physical parameters are affected by irradiation, such as minority carrier diffusion length (minority carrier lifetime) and base carrier concentration. Therefore, a detailed and useful analytical procedure to study the radiation damage in GaAs sub-cells should take into account the combined variations of these two parameters [5]. On the one hand, the reduction of the effective minority carrier lifetime (τ_{eff}) in the base layer of the devices is described by:

$$1/\tau_{eff} = 1/\tau_R + 1/\tau_{NR} \tag{1}$$

where τ_R and τ_{NR} are the radiative and non-radiative recombination lifetimes, respectively. The radiative recombination lifetime model includes the radiative recombination probability B and the base carrier concentration N and is expressed by:

$$1/\tau_R = B.N \tag{2}$$

whereas the non-radiative recombination lifetime degradation model caused by radiation-induced recombination centers is given by:

$$1/\tau_{NR} = \sum_i \sigma_i v_{th} N_{ri} = \left(1/\tau_\phi - 1/\tau_0\right) = K\phi \tag{3}$$

where τ_0 and τ_ϕ are the minority carrier lifetime before and after irradiation, respectively, σ_i is the captured cross section of the minority carrier by the ith recombination center, v_{th} is the thermal velocity of the minority carrier, N_{ri} is the concentration of the ith recombination center, K is the damage constant for the minority carrier lifetime and ϕ is the accumulated electron fluence.

On the other hand, the carrier removal effect in the base layer can also be caused by radiation-induced defects at high fluence. The decrease of the base carrier concentration with electron fluence can be described by:

$$\rho_\phi = \rho_0 . \exp\left(-R_C . \phi/\rho_0\right) \tag{4}$$

where ρ_0 and ρ_ϕ are the base carrier concentration before and after irradiation, respectively, and R_C is the carrier removal rate.

3. Simulation setup

The numerical analysis of the p-on-n and n-on-p GaAs structures with an area of 1×1 cm^2 has been performed in the optical device simulator PC1D for the AM0 spectrum. The p-emitter (0.5 μm) was doped at levels of 4×10^{17}, 8×10^{17} and 2×10^{18} cm^{-3}, and the n-base (3 μm) was contaminated at levels that varied from 9×10^{15} to 2×10^{17} cm^{-3}, whereas the n-emitter (0.15 μm) was doped at levels of 5×10^{17}, 1×10^{18} and 2×10^{18} cm^{-3}, and the different carrier concentrations varied from 2×10^{16} to 3×10^{17} cm^{-3} and were considered for the p-base (3 μm) region of the simulated devices. The Gaussian doping profiles were considered in all of the cases. The physical parameters described in table 1 have been used in the simulation.

The radiation damages were studied for 1 MeV electrons at fluences up to 4×10^{15} cm^{-2}, which are the major cause of degradation in the space solar cells' performance in geostationary Earth orbit (GEO) [14]. The value of B used in expression (2) is 2×10^{-10} $cm^3 s^{-1}$ [5]. In expression (3), the values of K were determined using:

$$K = K_L \cdot D \tag{5}$$

where K_L is the damage constant for the minority carrier diffusion length, and D is the minority carrier diffusion coefficient. The values of K_L for the n-GaAs and p-GaAs with 1 MeV of electron irradiation as a function of the initial base carrier concentration were determined by a theoretical fit to the experimental data presented in [15], as can be seen in figure 1. Finally, the carrier removal rate R_C for GaAs used in expression (4) is 5 cm^{-1} [16].

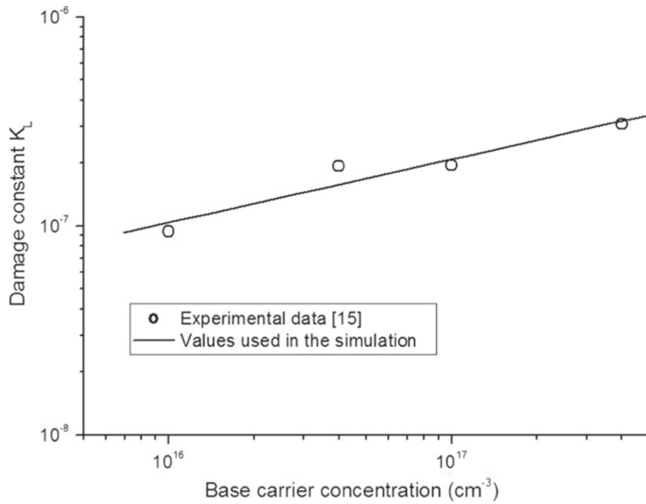

Figure 1. Changes in the damage constant for the minority carrier diffusion length in GaAs determined with 1 MeV electron irradiation as a function of the base carrier concentration.

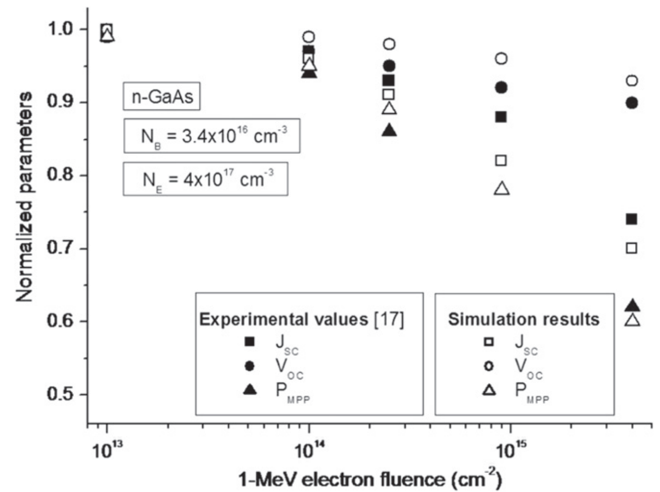

Figure 2. Normalized electrical parameters vs. fluence for the p-on-n GaAs sub-cell. The simulation results are in agreement with the experimental values.

4. Results and discussion

Figures 2 and 3 show the variation in the electrical parameters of the solar cell (short-circuit current J_{SC}, open-circuit voltage V_{OC} and P_{MPP}) as a function of the 1 MeV electron fluence for the n-GaAs and p-GaAs sub-cells, respectively. In figure 2, the p-on-n GaAs structure has been simulated with values of both the base and emitter carrier concentration of $N_B = 3.4 \times 10^{16}$ cm^{-3} and $N_E = 4 \times 10^{17}$ cm^{-3}, respectively. In contrast, the values of $N_B = 3.28 \times 10^{16}$ cm^{-3} and $N_E = 5 \times 10^{17}$ cm^{-3} have been used for the simulation of the n-on-p GaAs sub-cell in figure 3. For both values, the values presented are normalized to those that correspond to the non-irradiated devices.

The simulation results (curves with empty symbols) are in good agreement with the experimental values (filled symbols) extracted from [17]. Also, it can be verified that P_{MPP} is the electrical parameter most strongly affected under electron or proton irradiation [18, 19].

The results of the degradation in the P_{MPP} after electron irradiation are shown in figure 4 for n-type (curves with filled symbols) and p-type (empty symbols) GaAs sub-cells with a fixed N_E value in each case and for different N_B values from 9×10^{15} to 3×10^{17} cm^{-3}. Only a few curves were plotted in this graphic for clarity. The presented values are normalized to the initial value obtained before irradiation. It can be seen how radiation tolerance is a function of solar cell configuration. The best radiation tolerance for the n-GaAs sub-cells as well as for the p-GaAs sub-cells in the range of the studied design parameters is found when the lowest base carrier concentration is considered. Similar results have been obtained from [18].

In order to fully understand the degradation in the maximum power point induced by high fluence 1 MeV electron irradiation for different base and emitter carrier concentrations, it is important to consider the $P_{MPP}(\phi)/P_{MPP}(0)$ ratio,

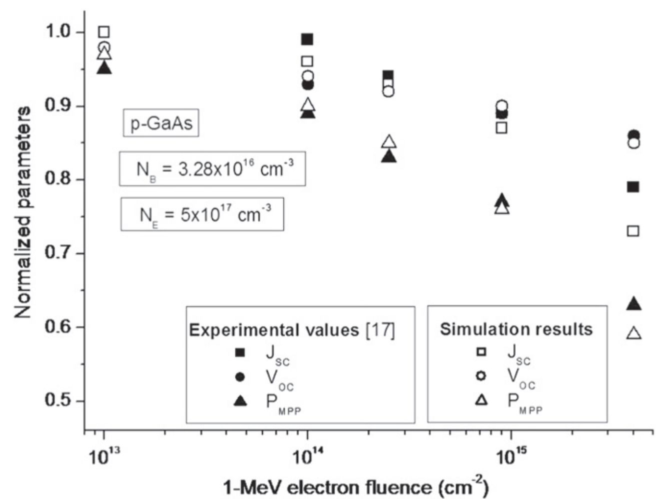

Figure 3. Normalized electrical parameters vs. fluence for the n-on-p GaAs sub-cell. The simulation results are in agreement with the experimental values.

where $P_{MPP}(0)$ and $P_{MPP}(\phi)$ are the maximum power points before and after irradiation, respectively. Figure 5 shows this ratio as a function of the base carrier concentration for a given electron fluence of $\phi = 4 \times 10^{15}$ cm^{-2}. Different emitter carrier concentrations have been analyzed. Curves with filled symbols correspond to the n-GaAs solar cells, whereas empty symbols correspond to the p-GaAs structures.

Tables 2 and 3 summarize the values of the $P_{MPP}(4 \times 10^{15}$ cm$^{-2})/P_{MPP}(0)$ ratio with a minimum and maximum N_B analyzed in this work for the n-GaAs and p-GaAs sub-cells, respectively. Specifically, for different N_E in the range of 4×10^{17} to 2×10^{18} cm^{-3}, the $P_{MPP}(\phi)/P_{MPP}(0)$ ratio decreases between 20 and 29% for the n-type GaAs when N_B is increased from 9×10^{15} to 2×10^{17} cm^{-3}.

Similarly, for p-type GaAs when N_B is increased from 2×10^{16} to 3×10^{17} cm^{-3}, the $P_{MPP}(\phi)/P_{MPP}(0)$ ratio

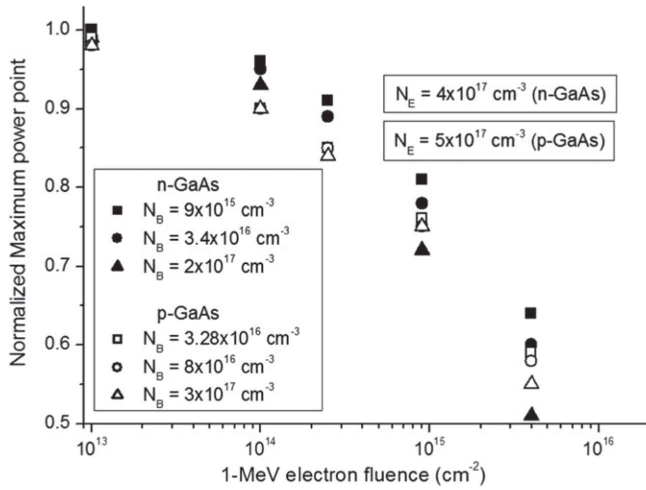

Figure 4. Degradation in the maximum power point of the GaAs structures as a function of 1 MeV electron fluence for different base and emitter carrier concentrations.

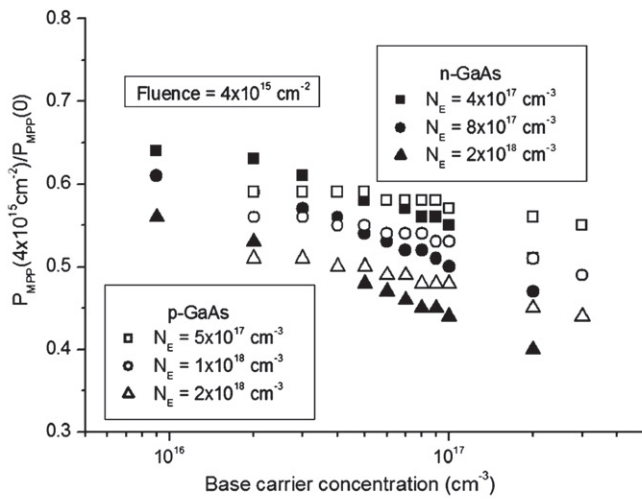

Figure 5. $P_{MPP}(\phi)/P_{MPP}(0)$ ratio against the base carrier concentration at $\phi = 4 \times 10^{15}$ cm^{-2}. Different emitter carrier types and concentrations were studied.

decreases between 7 and 14% for different N_E in the range of 5×10^{17} to 2×10^{18} cm^{-3}.

It can be observed in tables 2 and 3 that when the devices (p- and n-type) are exposed to the irradiation of high energy particles, the best performance is obtained when both the lowest base and the lowest emitter carrier concentrations are considered. However, a given solar cell, regardless of its structural characteristics, will have a satisfactory response to radiation for a specified time, during which it is possible to ensure that the electrical parameters of the device (J_{SC}, $V_{OC}$and P_{MPP}) will be kept above 80% of their non-irradiated values. This operation time is related to electron fluence and energy. In the previous work, 80% was also chosen as the reference degradation level of P_{MPP} [8].

From an interpolation of curves similar to those presented in figure 4 for the entire range of N_B and N_E considered in this paper, the highest fluence has been calculated in order to prevent the $P_{MPP}(\phi)/P_{MPP}(0)$ ratio from becoming lower than 0.8. This fluence has been named by the authors as ϕ_{80} in [12]. Figures 6 and 7 show the overall results obtained for the n- and p-type GaAs sub-cells, respectively, together with a first-order fit expressed in equation (6):

$$\phi_{80} = r.N_B + \phi\left(N_E\right) \quad (6)$$

where r is the rate of change of the ϕ_{80} fluence with respect to the N_B base doping concentration (expressed in cm^{-2}/cm^{-3} = cm), and $\phi(N_E)$ is the value of the ϕ_{80} fluence for very low values of the base doping concentration ($N_B \ll 9 \times 10^{15}$ cm^{-3})—in other words, when the curves are flattened. A theoretical fit, which includes the effects of the $N_E$emitter doping concentration, is given by $\phi(N_E) = a_1 + a_2.\log(k.N_E)$, where $k = 5 \times 10^{-19}$ cm^3 is the inverse of the maximum emitter doping concentration considered in the simulations. Equation (6), and therefore, the parameters r, a_1, a_2 and k, are valid for the range of the p-on-n and n-on-p GaAs structures, such as those described in the section 3.

Table 4 contains the constant values for expression (6) for the n- and p-type GaAs sub-cells. This analytical model is

Table 2. $P_{MPP}(\phi)/P_{MPP}(0)$ ratio for irradiated n-GaAs solar cells with $\phi = 4 \times 10^{15}$ cm^{-2}.

N_E (cm^{-3})	$P_{MPP}(\phi)/P_{MPP}(0)$ (for $N_B = 9 \times 10^{15}$ cm^{-3})	$P_{MPP}(\phi)/P_{MPP}(0)$ (for $N_B = 2 \times 10^{17}$ cm^{-3})	Decrease (%)
4×10^{17}	0.64	0.51	~20
8×10^{17}	0.61	0.47	~23
2×10^{18}	0.56	0.40	~29

Table 3. $P_{MPP}(\phi)/P_{MPP}(0)$ ratio for irradiated p-GaAs solar cells with $\phi = 4 \times 10^{15}$ cm^{-2}.

N_E (cm^{-3})	$P_{MPP}(\phi)/P_{MPP}(0)$ (for $N_B = 9 \times 10^{15}$ cm^{-3})	$P_{MPP}(\phi)/P_{MPP}(0)$ (for $N_B = 2 \times 10^{17}$ cm^{-3})	Decrease (%)
5×10^{17}	0.59	0.55	~7
1×10^{18}	0.56	0.50	~11
2×10^{18}	0.51	0.44	~14

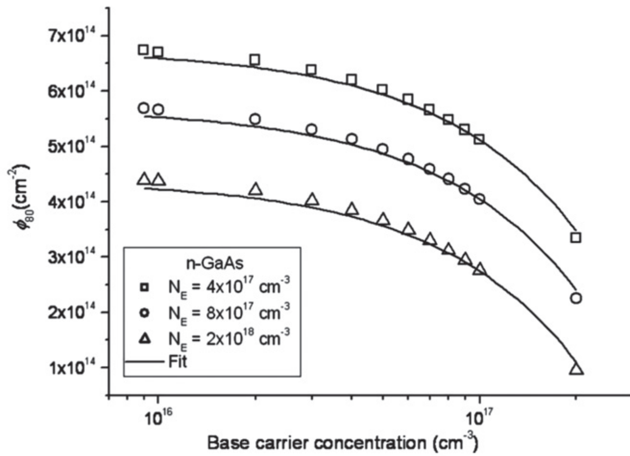

Figure 6. ϕ_{80} decay with increasing N_B and N_E from the simulations (symbols) and the fit (lines, equation (6)) for all of the studied n-GaAs sub-cells.

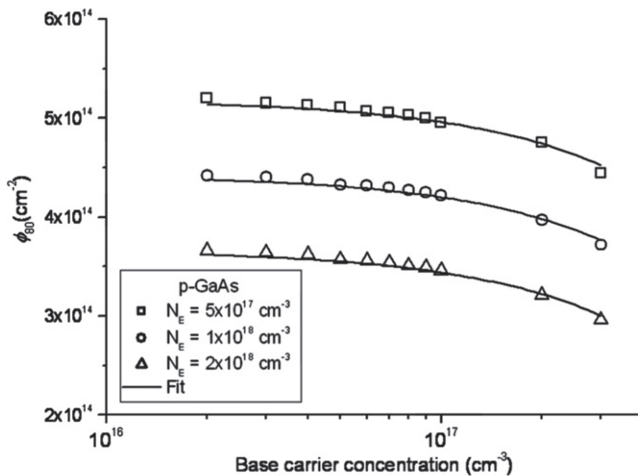

Figure 7. ϕ_{80} decay with increasing N_B and N_E from the simulations (symbols) and the fit (lines, equation (6)) for all of the studied p-GaAs sub-cells.

Table 4. Constant values for expression (6).

Constant	n-type GaAs	p-type GaAs
r	-1.79×10^{-3} cm	-2.5×10^{-4} cm
a_1	4.55×10^{14} cm^{-2}	3.71×10^{14} cm^{-2}
a_2	-3.36×10^{14} cm^{-2}	-2.52×10^{14} cm^{-2}

sufficiently robust to handle a broad range of N_B and N_E and gives good validity to the equation.

Expression (6) is useful to determine the highest electron fluence to which the electrical parameters of the solar cell, with well-known base and emitter carrier concentrations, are reduced simultaneously by less than 20% from their non-irradiated values. Additionally, the previous knowledge of the orbital location of the devices (altitude and inclination), together with the electron flux, would allow the determination of the maximum exposure time and the solar cell with the most suitable combination of N_B and N_E to enhance the radiation tolerance of the devices. Table 5 shows a comparison for ϕ_{80} between the two values obtained from expression (6) and the experimental data from [17] for 1 MeV electron of irradiated solar cells.

For example, for an n-type GaAs sub-cell with $N_B = 3.4\times10^{16}$ cm^{-3}, the analytical result calculated by the proposed theoretical fit indicates that for an electron fluence of $\phi_{80} = 6.25\times10^{14}$ cm^{-2}, the maximum N_E in order to keep the values of J_{SC}, V_{OC} and P_{MPP} above 80% of their pre-irradiation values is $N_E = 4\times10^{17}$ cm^{-3}. This fluence is equivalent to an exposure time at a geostationary orbit of nearly four years.

5. Conclusion

A theoretical study of the electrical performance of p-on-n and n-on-p GaAs sub-cells under AM0, irradiated with 1 MeV electrons at fluences below 4×10^{15} cm^{-2}, has been carried out by means of a computer simulation. These devices dominate the irradiation tolerance of the InGaP/GaAs/Ge 3J solar cells. The results obtained show how radiation tolerance is a function of the solar cell doping concentration. The highest maximum power point is obtained when both the lowest base and the lowest emitter carrier concentrations are considered. An analytical model related to the design parameters of the GaAs sub-cells, such as polarity and the doping concentration in the base and emitter regions, has been proposed. This model is useful to either determine the maximum exposure time or select the appropriate device in order to ensure that the electrical parameters of different GaAs sub-cells will have a satisfactory response to radiation since they will be kept above 80% with respect to the non-irradiated values.

Acknowledgments

This work was partially supported by the Universidad Nacional de La Plata (UNLP), Argentina, under Grant I-158;

Table 5. Theoretical fit and comparison with experimental data from [17].

N_B (cm^{-3})	N_E (cm^{-3})	ϕ_{80} (cm^{-2}) (Fit)	ϕ_{80} (cm^{-2}) (Experimental data)
3.4×10^{16} (n-type)	4×10^{17}	6.25×10^{14}	$\sim6.3\times10^{14}$
3.28×10^{16} (p-type)	5×10^{17}	5.13×10^{14}	$\sim5.15\times10^{14}$

by the Universidad Nacional Arturo Jauretche (UNAJ), Argentina; and by the National Council Research (CONICET), Argentina, under Grant PIP-112-201001-00292.

References

[1] Claeys C and Simoen E 2002 *Radiation Effects in Advanced Semiconductor Materials and Devices* (Berlin: Springer)
[2] Benton E R and Benton E V 2001 *Nucl. Instrum. Methods Phys. Res. Sect.* B **184** 255–94
[3] Lu M *et al* 2013 *Nucl. Instrum. Methods Phys. Res. Sect.* B **307** 362–65
[4] Zhang X, Hu J, Wu Y and Lu F 2010 *Semicond. Sci. Technol.* **25** 035007
[5] Elfiky D *et al* 2010 *Japan. J. Appl. Phys.* **49** 121202
[6] Sato S *et al* 2009 *Sol. Energy Mater. Sol. Cells* **93** 768–73
[7] Stassinopoulos E G and Raymond J P 1988 *Proc. IEEE* **76** pp 1423–42
[8] Sumita T *et al* 2003 *Nucl. Instr. and Meth. Phys. Res.* B **206** 448–51
[9] Wang R, Liu Y and Sun X 2008 *Nucl. Instrum. Methods Phys. Res. Sect.* B **266** 745–49
[10] Cappelletti M A, Cédola A P and Peltzer y Blancá E L 2008 *Semicond. Sci. Technol.* **23** 025007
[11] Cédola A P, Cappelletti M A, Casas G and Peltzer y Blancá E L 2011 *Nucl. Instrum. Methods Phys. Res. Sect.* A **629** 392–95
[12] Cappelletti M A, Casas G, Cédola A P and Peltzer y Blancá E L 2013 *Semicond. Sci. Technol.* **28** 045010
[13] PC-1D [available online at http://engineering.unsw.edu.au/energy-engineering/pc1d-software-for-modelling-a-solar-cell]
[14] Lantratov V *et al* 2010 *Adv. Sci. Technol.* **74** 225–30
[15] Yamaguchi M and Ando K 1988 *J. Appl. Phys.* **63** 5555–62
[16] Khan A, Yamaguchi M, Bourgoin J and Takamoto T 2002 *J. Appl. Phys.* **91** 2391–97
[17] Warner J *et al* 2005 *Proc. 8th European Conf. on Radiation and its Effects on Components and Systems (RADECS 2005)* 1PG5-1–6
[18] Yamaguchi M *et al* 2006 *Proc. 4th IEEE World Conf. on Photovoltaic Energy Conversion* 2 pp 1789–92
[19] Makham S, Zazoui M, Sun G and Bourgoin J C 2006 *Sol. Energy Mater. Sol. Cells* **90** 1513–18